CONFERENCE PRE-PRINT

ANALYSIS OF BACKGROUND PLASMA BEHAVIOR UNDER EXTERNAL FIELDS IN THE LOW ENERGY BEAM TRANSPORT SECTION OF LIPAC

[1]T. ITAGAKI, and [1-5]IFMIF/EVEDA Integrated Project Team

[1]QST-Rokkasho, Aomori, Japan
[2]CEA Paris-Saclay, Gif sur Yvette, France
[3]INFN, Legnaro, Italy
[4]Fusion for Energy, Garching, Germany
[5]IFMIF/EVEDA Project Team, Aomori, Japan

Email: itagaki.tomonobu@qst.go.jp

Abstract

Background plasma behaviour in the low energy transport section of the LIPAc is analysed with 3-dimensional particle-in-cell simulation. The simulation showed some characteristic effect under external field elements in the LEBT: a positive biased chopper absorbed the electron plasma in the surrounding drift region, that is limited by the solenoid lenses, though indicating some electron leakage through the solenoid still be there. Analytically estimated flux of the electron leakages through solenoid is compared to the simulation results. Results of experiments still has a mysterious transient motion of beam pulse shape that is not shown in the simulations, while saturated state is roughly reproduced in it.

INTRODUCTION

The International Fusion Materials Irradiation Facility (IFMIF) is an accelerator-driven intense neutron source using D-Li nuclear reaction for irradiation of potential candidate materials constituting a fusion DEMO reactor, and now the Engineering Validation and Engineering Design Activity (EVEDA) phase is ongoing under the Broader Approach (BA) agreement between Japan and the EU [1]. The Linear IFMIF Prototype Accelerator (LIPAc) is under commissioning progressively in several phases in Rokkasho, Aomori, Japan. The mission of LIPAc is to validate the acceleration of a deuteron beam of 125 mA to 9 MeV in continuous wave (CW) mode. A commissioning phase of the LIPAc called “Phase B+ has been held in 2021-2024, whose main objective was to validate the deuteron beam acceleration by RFQ up to 5 MeV at a high-duty cycle and to characterize the beam. The main outcomes of Phase B+ stage 1 (pilot beams using proton/deuteron beam) were reported at FEC2023 [2], and the outcomes of whole the Phase B+ is to be reported in FEC2025 [3].

1. LIPAC INJECTOR

An injector composed with an ECR ion source, and a low energy beam transport (LEBT) line with 2.05 m of its length is on the top of LIPAc beam line. Fig. 1 shows the configuration of LIPAc injector. The LEBT is mainly composed with two solenoid lenses (SOL1, 2) with steering magnets (ST1, 2) to guide and focus the beam up to the RFQ entrance, a beam stopper (FC), an emittance measurement unit (EMU), and an electrostatic chopper to kick the beam vertically for short-pulsed operations. Five electrodes are used to extract deuterium or proton beams from the ECR ion source. The intermediate electrode installed between the plasma and grounded electrode has a role to adjust extracted beam profile. The repeller electrode placed between the two grounded electrodes is applied negatively so that reflects backflow electrons from the LEBT. The specifications required for the beam extraction are shown in Table 1.

Subcomponents of the extracted beam such as molecular ion beams have a smaller specific charge than the main beams so that they can be removed on an exit cone of LEBT as they will not be focused by the solenoid lenses at there. Another repeller electrode is placed at the end of the exit cone to prevent electrons from entering the RFQ. The RFQ injection current is measured by a Current Transformer (ACCT) at the exit of the LEBT. In addition, an optional mechanism to inject krypton gas into the LEBT, to accelerate space charge compensation that will be described in the next chapter.

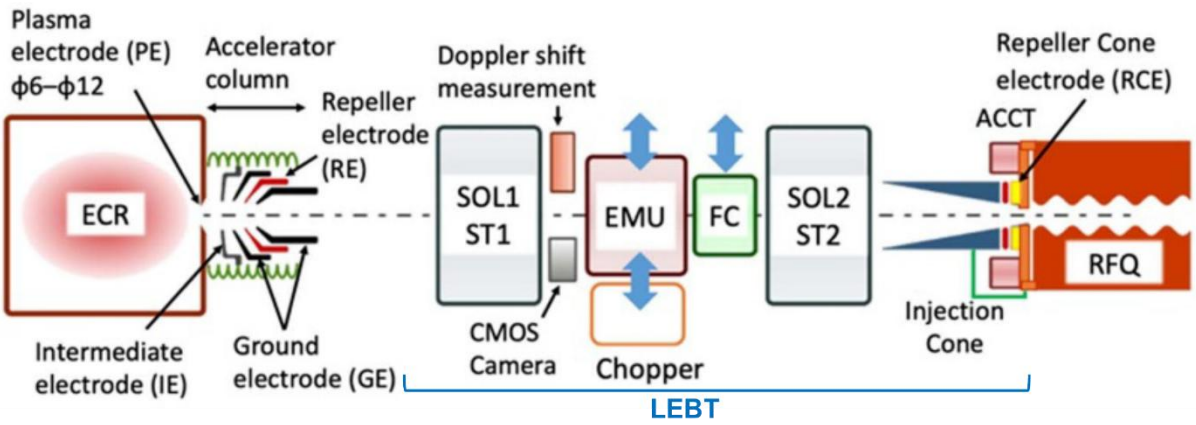

FIG. 1. Configuration of LIPAc Injector

TABLE 1. REQUIREMENTS FOR THE LIPAC INJECTOR

	D^+	H^+
Beam energy (keV)	100	50
Beam current (mA)	140	70
RMS emittance	< 0.25	< 0.25
(π.mm.mrad)	(0.3 acceptable)	(0.3 acceptable)
Operation mode	Pulse/CW	Pulse

2. SPACE CHARGE COMPENSATION IN THE LEBT

Accurate prediction of beam behaviour in the injector is crucial for safe commissioning without critical beam losses since it dominates the accuracy of beam prediction of whole the LIPAc. Background plasma in LEBT, generated by ionization of residual gas or secondary electron from beam loss, affects the beam by neutralizing its space charge force. This effect, known as space charge compensation (SCC) [4], is significant due to the high beam density in there. When conducting short pulse operations on the order of 100 us using the chopper, the time scale on the SCC develops is close to that on the beam pulse so that predicting the time evolution of SCC is important for the smooth progress of the commissioning. Fig. 2 shows the results of the Kr gas injection tests using a proton beam in 2021. The beam pulses have characteristic two-stepped shapes, and their middle step were shortened depending on the amount of Kr gas injected, while the flat region in the latter side expanded.

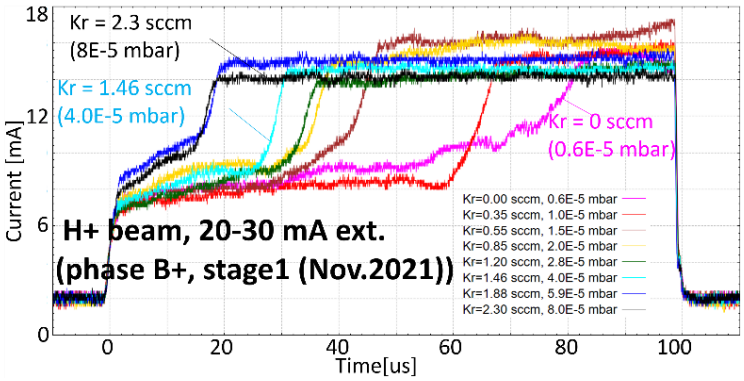

FIG. 2. Beam pulses related to Kr injection observed in the LIPAc commissioning in 2021.

3. SIMULATION FOR SCC IN LIPAC LEBT

This study is devoted to a simulation and an analytical modelling of a part of plasma behaviour to enable accurate beam prediction. To understand the effects of external fields on the plasma and the SCC in the LEBT,

we performed a three-dimensional particle-in-cell (PIC) simulation to simulate details of the plasma behaviour of during whole transient and steady state since its analytical models are still limited like ones assuming steady state of a beam in a drift space without any external fields [5,6]. The simulation code is based on Warp [7] and is controlled by self-made input codes. The simulation used the estimated profile of the proton beam from Phase B+ stage 1 commissioning, shown in Fig. 3. The total extracted beam current was around 22 mA, including its 30 % H_2^+ subcomponent beam, under a background H_2 gas pressure of 1.2×10^{-5} mbar. Fields on SOL1,2 centres are 0.185 and 0.217 T. The simulation tracked the "kicked" beam using the chopper for 200 μs to reach a steady state, followed by 100 μs after the chopper was turned off. Particle species and reactions used in the simulation is shown in Table 2. Electrons and H_2^+ ions from gas ionization by beam-gas collisions are used as background plasma particles. The background H_2^+ ions mentioned above and the secondary electrons from the beam pipe by beam loss are optionally able to be included, while the most part of detailed analysis described in the next chapter is focused on the case in which the wall secondary emission is neglected for simplicity.

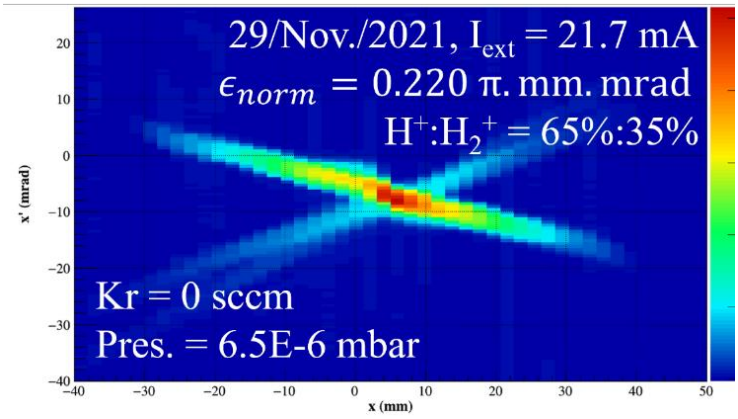

FIG. 3. Extracted beam profile measured on the EMU.

TABLE 2. PARTICLES AND REACTIONS INCLUDED IN THE SIMULATION

Particles	Particle source	Reactions
H^+ H_2^+	Beam extraction	$H^+ + H_2\ \text{gas} \rightarrow H_2^+(\text{ionization}) + e^-(\text{ionization})$ $H_2^+ + H_2\ \text{gas} \rightarrow H_2^+(\text{ionization}) + e^-(\text{ionization})$ $H^+ + \text{wall} \rightarrow e^-(\text{wall secondary},\ \text{SEY} = 1.3)$ $H_2^+ + \text{wall} \rightarrow e^-(\text{wall secondary},\ \text{SEY} = 2.6)$ (SEY: secondary emission yield)
e^- H_2^+(optional)	Background gas ionization	
e^-(optional)	Secondary emission from beam pipe wall	

4. RESULTS AND DISCUSSION

4.1. Characteristic features of neutralization and BG plasma

Fig. 4 shows the simulation results of the case with neglecting wall secondary emission, including the line density distributions normalized to that of injected proton beam along the beam axis under steady state with the chopper being on as Fig. 4(a) and off as Fig. 4(b). When the chopper is on, the background plasma particles in the drift space around the chopper are removed as seen in Fig. 4(a), and the solenoid lenses spatially limited the chopper's effect with their plasma confinement effect. After the chopper turned off, around the chopper, the beam is defocused by its space charge force until the background plasma fulfilled, and this will dominates rise time of effective beam pulse. Changes of the background electron density in the drift space at the upstream side of the first solenoid between Fig. 4(a) and (b) indicates some remaining leakage path through the solenoid. Fig. 5 shows time evolution of the SCC rate in the same case along the beam axis obtained from ratio of line density of charge in background plasma to that in the beams, with 15 us step after chopper turned off from the steady state shown in Fig. 4(a). The 0 % case in Fig. 5 means no SCC effect so that the beam is fully exposed to its own space charge force. Since the estimated rising rate of the neutralization is around 2 %/us due to the ionization and smaller than

the result seen in Fig. 5, we speculated that there would be some leakage through the axis of the solenoid where its radial field is so small that it cannot reflect electrons.

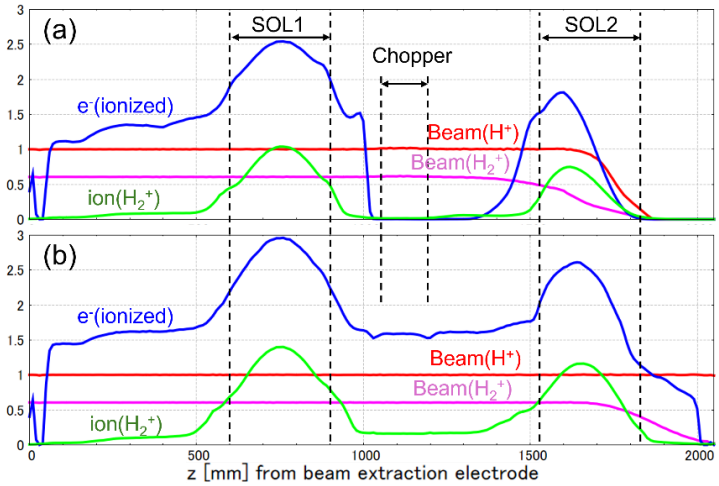

FIG. 4. Linear number densities in the simulation under steady state with chopper is (a) turned on, and (b) turned off.

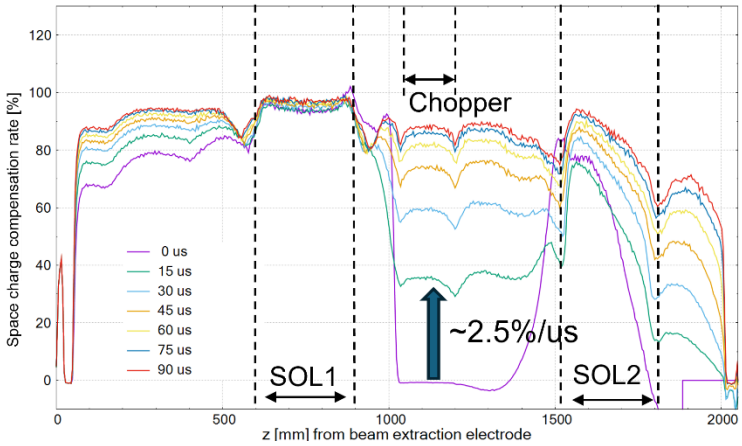

FIG. 5. Time evolution of SCC rate along beam axis after the chopper turned off.

4.2. Estimation of electron plasma leak through the solenoids

We tried to estimate the area of this leakage channel roughly, based on the relationship between the magnetic and electrostatic fields. Assuming there is a leak channel of a certain radius from the centre of the solenoid to the edge on the chopper side. let E_z, B_r be the averages of axial electric field and radial magnetic field, that the electron fluid experiences as it passes through the channel, and time derivative $\nabla_t = d/dt$, equation of motion is as follows.

$$m_e \nabla_t u_\theta = -e u_z B_r$$
$$m_e \nabla_t u_z = -e(E_z - u_\theta B_r)$$

where $u_s(s = \theta, z)$ is the flow velocity of the electrons. By integrating the first equation twice over time with assuming initial state as $v_\theta(0) = 0$ and $\frac{d}{dt} v_\theta(0) = 0$, we obtain a equation as follows.

$$\int_0^T u_\theta \, dt = -\frac{e}{m_e} B_r T \Delta z$$

where Δz and T are the channel length and the time it takes for an electron to pass through the channel. Considering electrons on the radial edge of the channel, their z-direction velocity becomes zero just as they pass through the channel, so substituting this into the time-integrated second equation above gives the following equation:

$$0 = m_e u_{z0} - e E_z T - \frac{e^2 B_r^2}{m_e} T \Delta z$$

where $u_{z0} = u_z(0)$. Considering that the magnetic flux penetrating the cross section of the beam pipe at the centre of the solenoid is equal to the magnetic flux penetrating the beam pipe wall on one side of the solenoid, the following can be substituted for B_r.

$$B_r = \frac{B_{z0} r_0}{2\Delta z}$$

where B_{z0} is B_z on the centre of solenoid. In addition, the potential difference between the entrance and exit of the channel is $\Delta\phi = -E_z \Delta z$, and if we assume roughly the u_z changes linearly, we predict that $\Delta z/T \approx u_{z0}/2$. With substituting them into the previous equation, the channel area πr_0^2 can be estimated as follows.

$$\pi r_0^2 \approx \frac{4\pi m_e}{e^2 B_{z0}^2}\left(\frac{m_e u_{z0}^2}{2} + e\Delta\phi\right)$$

Fig. 6 shows the distribution of electron flow velocity in the same simulation case to the Fig. 4 and 5, in which wall secondary emission is neglected, within the 1st solenoid just after the chopper is turned off. The electron flow velocity at the solenoid centre was 2.2×10^6 m/s, and the potential difference between the centre and its chopper-side edge was 88 V, and then the channel area was estimated as 0.23 mm^2. Multiplying this channel area by the flow velocity and the electron density for the beam at the solenoid centre shown in Fig. 4(b), we estimated the contribution in neutralization rate around the chopper due to electron flow toward the chopper through this channel to be 0.27%/μs. This estimated value seems to provide a good explanation for SCC improving rate around the chopper is approximately 0.5% higher than the value that predicted from gas ionization, even same approach was difficult for the 2nd solenoid since the beam was still off-axis. The estimated channel radius is considerably smaller than the spread of the electron flow velocity that indicates most electrons were still captured in the edge field of the solenoid. From this and the background ions concentrated around the solenoids shown in Fig. 4, practically for the view of beam optics, it seems to be good approximation that the space charge of the beams are fully neutralized in the solenoids, where quasi-neutral plasma was formed.

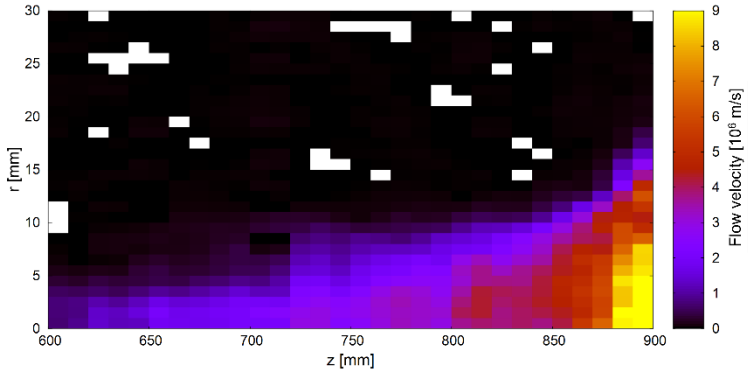

FIG. 6. Axial frow velocity distribution simulated in the 1st solenoid.

4.3. Comparison of simulation to the experiment

Fig. 7 shows a comparison of the beam pulse predicted by the simulation with the beam pulse observed without krypton injection. Fig. 7 also shows the results when changing the background particle species included in the simulation. The red line is the case that considers background gas ionization as analysed above; the green line considers secondary electron emission from the wall due to beam loss; and the blue line considers wall secondary electrons but ignores background ions from gas ionization. The characteristic two-step structure seen in experiments was not reproduced in either case unfortunately, but the beam current at the end of the pulse. Comparing the time evolution in these cases with the experiment, the cases in which wall secondary emissions were considered shows rapid rising at the first stage of the beam pulse, that is like that of the experiment. In the other hand, the time scale of the middle step in the case without wall secondary electrons is similar to that of the experiment. The result of the krypton injection test shown in Fig. 2 also agrees that the time scale of this middle step depends on that of background gas ionization. In contrast, the rise of the first step may be related to neutralization by the wall secondary electrons.

The fact that the two-step structure cannot be reproduced in the simulation suggests that processes not included in the current simulation have a significant impact on the transition of the background electron plasma. Energy transfer due to Coulomb collisions is a possible candidate. Energy transfer due to Coulomb collisions is a candidate, and the possible process is as follows. Just after chopper-off, the wall secondary electrons provide high-temperature electron plasma due to the potential energy where they generated, and then, gradually replaced to low-temperature electrons from gas ionization as the beam loss decreases. In the current simulation, the low-

temperature electrons are not heated by collisions to the high-temperature ones so that they can fill the remaining part of the potential well.

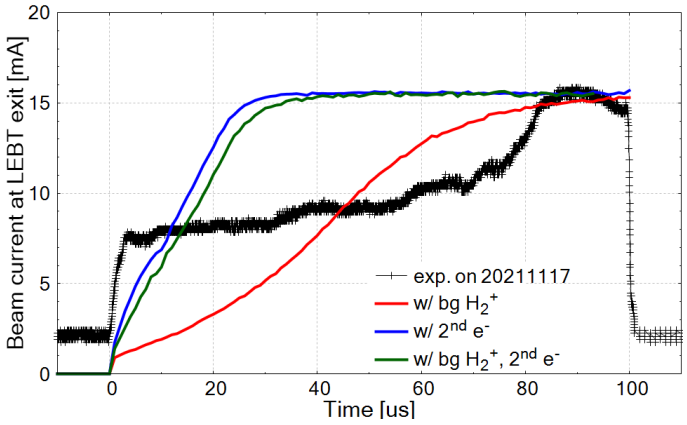

FIG. 7. Comparison of the RFQ injection beam pulse between the experiment and simulations.

Electrons are treated as particles in current simulations, that makes it difficult to include the Coulomb collisions from the view of calculation amount. Even if we use a method [8] that uses Monte Carlo scattering of particles through a spatial grid, the amount of calculation required would be about 10 times greater than that of current one. This is an unrealistic amount that requires more than a year for each case even using the supercomputer (JFRS-1) have been placed at QST-Rokkasho. A realistic way to include energy transfer to electrons through Coulomb collisions in a PIC simulation is to use a hybrid method, which treats electrons as a fluid represented on the spatial grid, however, this also requires to change the computational model largely.

5. SIMULATION MODEL UNDER DEVELOPMENT

To provide more fast and brief simulation that can track changes in the density, flow velocity, and temperature of the background electron plasma with considering Coulomb collisions naturally, we devised a model that treats electrons as a fluid distributed in one-dimensional space. A simulation code using this model are currently under development. In this model, electrons generated per unit time due to gas ionization and emission from the wall surface instantly exchange energy with surrounding electrons and become part of the electron fluid, and as a bit strong assumption for making the model one-dimensional, we assume that the Boltzmann distribution of the electron fluid also applies to the total mechanical energy, which is the sum of the kinetic energy and potential energy relative to the bottom of the potential well. Loss of electrons on the beam pipe are considered when they generated, and the loss rate is estimated from the part of electrons overwhelms the potential well as follows.

$$r = \exp\left(-\frac{e\phi}{k_b T_e}\right)$$

except in the region under the confinement by solenoid fields where we apply $r = 0$, where k_b is the Boltzmann constant, T_e is the electron temperature, and ϕ is the potential well depth. From continuity equation of electron fluid, we can obtain time derivative of electron density as follows.

$$\frac{\partial n_e}{\partial t} = (1 - r)g_e - \frac{\partial (n_e u_e)}{\partial z}$$

where g_e is electron production rate at there. For the next, with ignoring effect of momentum transfer collisions between the electrons and background gas since its mean free path is much larger than the LEBT length, we can obtain time derivative of electron flow velocity from equation of motion of the electron plasma as follows,

$$m_e n_e \frac{\partial u_e}{\partial t} = e n_e \frac{\partial \phi}{\partial z} - k_b \frac{\partial (n_e T_e)}{\partial z} - m_e n_e u_e \frac{\partial u_e}{\partial z}$$

where m_e is the electron mass. Finally, with ignoring correction of relativity, we can obtain time derivative of the temperature of electron fluid from the law of energy conservation as follows.

$$n_e k_b \frac{\partial T_e}{\partial t} = \mathcal{E}_{cc}(n_e) + \mathcal{E}_{ge} + \mathcal{E}_{pe}(\phi) - \left(\frac{1}{2} m_e u_e^2 + \frac{3}{2} k_b T_e - e\phi\right) \frac{\partial (n_e u_e)}{\partial z}$$

where $\mathcal{E}_{cc}$ is the term of energy transfer from beam to electron plasma by Coulomb collisions, and $\mathcal{E}_{ge}$, $\mathcal{E}_{pe}$ are terms of initial kinetic and potential energy of produced electrons. An equivalent model, which excludes terms of time derivative and flow from the last equation, was devised by Gabovich et al. [6] and introduced by Winklehner [5]. From these equations, we will be able to track time evolution of the density, flow velocity and temperature of the background electron plasma.

6. SUMMARY

The particle-in-cell simulation was performed to understand the time-transient behaviour of the background plasma and the SCC effect in the LIPAc LEBT. The simulation showed that the chopper removes background plasma significantly, while solenoids limit its effect, and this impacts on SCC. Electron leakage through solenoids was observed when the chopper was off. A theoretical estimation of the leak channel was performed, and it has good agreement with the simulation result.

A characteristic transient motion of beam pulses observed in the experiment was not reproduced in the simulation, but we could obtain some important knowledges to understand it. based on this, a new simulation that may be able to reproduce a possible mechanism is under development.

These knowledges about characteristics of background plasma and SCC provide the essential understanding for the accurate beam prediction in the next LIPAc beam commissioning phase so called “Phase C” and promise it to be safe and successful.

ACKNOWLEDGEMENTS

This study is performed with supports of the IFMIF/EVEDA Integrated Team, under the Broader Approach (BA) agreement between Japan and the EU.

REFERENCES

[1] Y. Carin, et al., Overview of Achievements of the IFMIF/EVEDA Project, proceedings of FEC2023, IAEA-CN-316-1681 (2023).

[2] K. Masuda, et al., Beam Commissioning of Linear IFMIF Prototype Accelerator (LIPAc) Toward High-Duty Operation at 5 Mev, 125 mA D+, 29th IAEA Fusion Energy Conference (FEC2023), TEC-FNT/P1-1741.

[3] T. Akagi, et al., Accomplishment of High Duty Cycle Beam Commissioning of Linear IFMIF Prototype Accelerator (LIPAc) at 5 MeV, 125 mA D+, 30th IAEA Fusion Energy Conference (FEC2025)

[4] N. Chauvin, et al., Transport of intense ion beams and space charge compensation issues in low energy beam lines, Rev. of Sci. Instrum. 83, 02B320 (2012).

[5] D.Winklehner and D.Leitner, A space charge compensation model for positive DC ion beams, JINST 10 (2015) T10006.

[6] M. Gabovich, et al., Self-decompensation of a stable quasi-neutral ion beam due to coulomb collisions, Fiz. Plazmy 1 (1975) 304.

[7] D.P. Grote, et al., The WARP code: Modeling high intensity ion beams, AIP Conf. Proc. 749 (2005) 55.

[8] W. M. Manheimer, et al., Langevin Representation of Coulomb Collisions in PIC Simulations, J. Comput. Phys. 138, 563–584 (1997)